Transmission properties of frequency selective structures with air gaps*

Meng Zhi-Jun(蒙志君)†, Wang Li-Feng(王立峰),
Lü Ming-Yun(吕明云), and Wu Zhe(武 哲)

School of Aeronautic Science & Engineering, Beihang University, Beijing 100191, *China*

(Received 2 May 2010; revised manuscript received 24 June 2010)

The transmission properties of compound frequency selective structures with dielectric slab and air gaps were investigated by computation and experimentation. Mechanism analyses were also carried out. Results show that the air gaps have a distinct influence on the transmission properties. Resonant frequency of the structure would increase rapidly when the air gap appears. After the gap gets larger to a specific value, generally 1/5 wavelength corresponding to the resonant frequency, the transmission properties would change periodically with the gap thickness. The change of transmission properties in one period has a close relationship with the dielectric thickness. These results provide a new method for designing a bandpass radome of large incidence angle and low loss with the concept of stealth shield radome.

Keywords: air gap, frequency selective structure, periodic array, radome

PACC: 7300

1. Introduction

Frequency selective surfaces (FSSs) are spatial filters that are typically used in high performance radomes for radars and antennas. The bandpass FSS structures comprise a series of aperture elements embedded in one or several metallic screens which are loaded by dielectric. They can pass the electromagnetic wave in certain frequency ranges and shield others, which are especially suitable for out-of-band stealth of radomes.[1−5]

Experimentation is an important means of studying FSS, but experimentative studies are usually limited.[6,7] For example, the dielectric thickness is constant or cannot vary much. In order to make a further research into dielectric properties, it is an effective way to adopt the adhesive FSS film. FSS films are separately manufactured; then they are made adhere to dielectrics of different properties. The advantage is that the FSS films and dielectric substrates can be repeatedly used, therefore the systematic experiments could be conducted.[8] The influence of adhering way cannot be ignored when the film adheres to the dielectric. In general test, the adhesive layer is not used when the FSS film adheres to the dielectric substrate. Instead, the corners or edges of FSS film are sticked to the dielectric slab by adhesive tapes, which probably results in air gaps. In the experiment, it shows that the influence of air gap is so strong that the transmission properties of FSS structure are even radically changed.

In this paper, the slot array is taken as an example. A deep research is carried out into the air gaps in compound structures of adhesive FSS films and dielectric slabs. The well developed modal matching method[9] is applied to make the calculation and analyses, partly associated with experimentation. In addition, further mechanism analysis would also be performed.

2. Model and method

2.1. FSS structure with air gaps

The FSS structure is shown in Fig. 1(a). A gap of air exists between the FSS film and the dielectric slab. The FSS film is a thin film structure of adhesiveless polyimide (PI) sheet covered by copper. The copper foil is so thin that it can be considered as the infinitely thin perfect conductor in microwave band. The gap thickness $d_{\rm air}$ will be actively changed in order to study the influence of air gaps. Figure 1(b) presents the geometric parameters and the incidence condition of the slot array.

*Project supported by the Major Research Plan of the National Natural Science Foundation of China (Grant No. 90305026).
†Corresponding author. E-mail: mengzhijun@buaa.edu.cn
© 2010 Chinese Physical Society and IOP Publishing Ltd

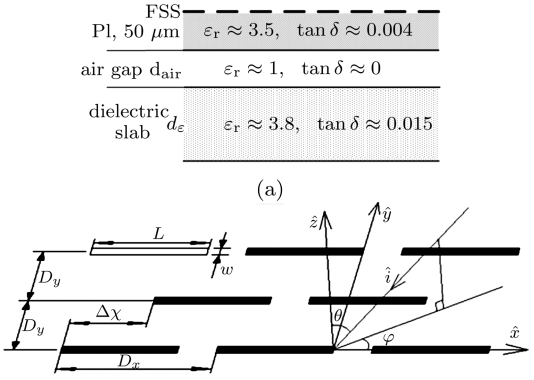


Fig. 1. Sketch map of the FSS structure and slot array. (a) FSS structure with air gaps. (b) Geometric parameters of slot array.

Since films are made of flexible material, FSS apertures are made by photochemical etching on the copper sheet using printed circuit technique which has been well developed.[8,10]

2.2. Calculation and experimentation

Modal matching method, elaborated in a number of literatures,[8] is a kind of moment method. The electric fields in all areas are expanded to Floquet modes, with continuous boundary condition at the interfaces. The integral equation describing the frequency response can be derived, whose unknown variables are the tangential electric fields,

$$\sum_{r=1}^{2}\sum_{pq}(Y_{pqr}^{1}+Y_{pqr}^{(1)})\boldsymbol{\psi}_{pqr}\iint_{S}\boldsymbol{E}_{\mathrm{t}}\cdot\boldsymbol{\psi}_{pqr}^{*}\,\mathrm{d}s = 2\sum_{r=1}^{2}\left(A_{00r}\xi_{00r}\prod_{k=1}^{N}U_{00r}^{k}\psi_{00r}\right), \quad (1)$$

where p and q are the Floquet modes due to the periodicity of the array, r refers to TE or TM mode, ψ is the vector Floquet mode function, ξ_{00} is the admittance of free space, A_{00} is the incidence coefficient, $\boldsymbol{E}_{\mathrm{t}}$ is the tangential electric field in apertures, S is the aperture area, Y_{pqr}^{1} and $Y_{pqr}^{(1)}$ respectively refer to the equivalent admittance from FSS to the directions of $-\hat{z}$ and $+\hat{z}$. Method of moment is applied to solve the integral formula (1). The tangential electric fields are expressed by a set of basis functions. After the weighting coefficients of the basis function have been solved, transmission and reflection coefficients therefore could be finally obtained based on transmission line theory.

The experimentation is also performed in the microwave anechoic chamber. In the experiment, the sizes of FSS film and dielectric slab are both 600 mm×400 mm.

3. Analysis and discussion

3.1. Influence of air gaps

In the structure as shown in Fig. 1, the thickness of dielectric slab is set at d_{ε} = 8.2 mm. This thickness is about $\lambda_{\varepsilon}/2$ which corresponds to the resonant frequency 9.5 GHz of FSS film. Set the thickness of air gap at certain values between 0 and 60 mm, some of which are used in experiment.

Figure 2 shows the transmission curves of typical thicknesses at normal incidence, in which C_{T} means the transmission coefficient. With the air gap enlarged, the transmission curve shifts rightward, i.e., the resonant frequency gets higher, and correspondingly the insert loss gets smaller. When d_{air} varies among 0, 0.2 mm and 2 mm, the change in transmission curves is distinct. But the curve for d_{air} = 2 mm is quite close to that for d_{air} = 15 mm, which indicates that the change of transmission properties is getting slight as the air gap widens. As the test frequencies are limited in the range of 8–12 GHz, only the results of d_{air} = 2 mm and 15 mm are given. The bandwidths of the curves measured are a little wider than that by calculation, while they are in good agreement on the whole.

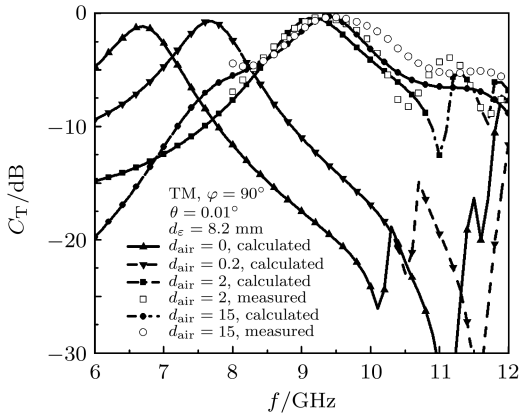


Fig. 2. Transmission curves of FSS structure with typical air-gap thicknesses.

Figure 3 provides more information about the influence of air gaps on resonant frequency when the gap varies in a large range below 60 mm. Three results of different dielectric slabs are given, whose thicknesses are 1 mm, 4.1 mm, and 8.2 mm respectively. Some

data of measurement at $d_\varepsilon = 8.2$ mm are also provided, and agree well with calculated results. In the three calculated curves, the resonant frequencies vary with the thickness of air gap in the same tendency. The resonant frequencies increase rapidly as $d_{\rm air}$ varies from 0 to $\lambda/30$. Compared with the case of no air gap, the resonant frequencies of $d_{\rm air} = 0.2$ mm are about 1 GHz higher, and about 2 GHz higher at $d_{\rm air} = 1$ mm. After $d_{\rm air}$ has increased to $\lambda/5$, the resonant frequencies are getting stable and changing at a period of $\lambda/2$.

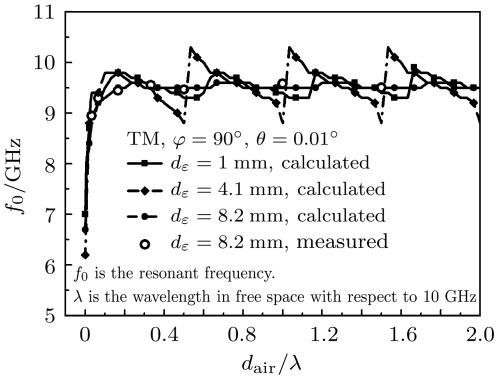


Fig. 3. Influence of air gaps on resonant frequencies.

The thickness of the dielectric slab d_ε also plays an important role. There are obvious differences of the three thicknesses shown in Fig. 3. The resonant frequency gets stable and maintains around the resonant frequency of FSS film (9.5 GHz) at $d_\varepsilon = 8.2$ mm, while the resonant frequencies of the other two thicknesses change rather violently. Therefore, whether it is sensible to the FSS loading effect depends on the thickness of dielectric slab when the air gap is large.

The influence of air gaps on transmission coefficients are illustrated in Fig. 4, in which $C_{\rm T0}$ means the in-band transmission coefficient at the resonant frequency. The results indicate that the in-band transmission coefficient changes with a period of $\lambda/2$ when $d_{\rm air}$ is larger than a certain value of about $\lambda/5$. The variation range of the coefficient is the largest when d_ε equals 4.1 mm, while it almost keeps constant at $d_\varepsilon = 8.2$ mm. The change at $d_\varepsilon = 1$ mm is between the above two cases. These phenomena agree with the changes of resonant frequencies shown in Fig. 3.

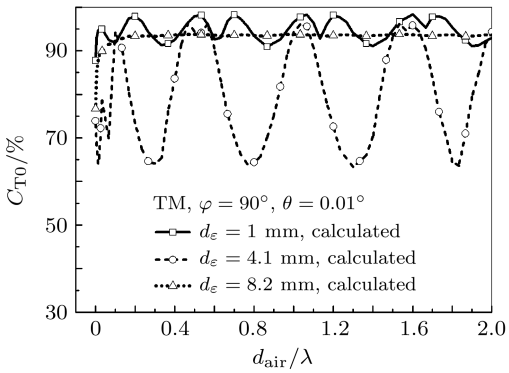


Fig. 4. Influence of air gaps on the in-band transmission coefficients. $C_{\rm T0}$ is the transmission coefficient at resonant frequency f_0, λ is the wavelength in free space with respect to 10 GHz.

3.2. Mechanism analysis of transmitted field

The mechanism can be investigated by analysis of transmitted fields of different Floquet modes. To simplify the issue, a slot array in free space is studied without the dielectric slab. The transmitted fields of the slot array can be easily obtained and expanded to all Floquet modes, described as a series of complex vectors

$$\dot{\boldsymbol{H}}_{\rm t}(\boldsymbol{R}) = \sum_k \sum_n \dot{\boldsymbol{H}}_{\rm t}(\boldsymbol{R}, k, n), \tag{2}$$

where $\boldsymbol{R}$ is an arbitrary point in the space of transmission side. If R_z is the distance from observation point to FSS array, $\boldsymbol{R}$ can be set at (0, 0, R_z). The normalized amplitude of the transmitted field of modes p and q is

$$T(\boldsymbol{R}, p, q) = 10 \cdot \lg \frac{|\dot{\boldsymbol{H}}_{\rm t}(\boldsymbol{R}, p, q)|}{|\dot{\boldsymbol{H}}_{\rm t}(\boldsymbol{R}, 0, 0)|}, \tag{3}$$

where $\dot{\boldsymbol{H}}_{\rm t}(\boldsymbol{R}, 0, 0)$ is the transmitted field of the principal mode (0, 0), equal to the incidence field $\dot{\boldsymbol{H}}_i$ at the resonant frequency. And according to Eq. (3), $T(\boldsymbol{R}$, 0, 0) is identical to 0 dB.

Figure 5 illustrates the distribution of $T(\boldsymbol{R}, p, q)$ with respect to Floquet modes p and q when R_z is 0.1, 0.2, 2 and 15 mm. It is in normal incidence, and the frequency is set at the resonant frequency. As shown in Fig. 5, the modes of transmitted field below –30 dB appear fewer and fewer when the observation point moves farther from the FSS array. Finally they converge towards the principal mode of (0,0) order. This is because only the principal mode of the spherical wave radiated from the slot array can be propagated while others are attenuated when there is no grating lobe.

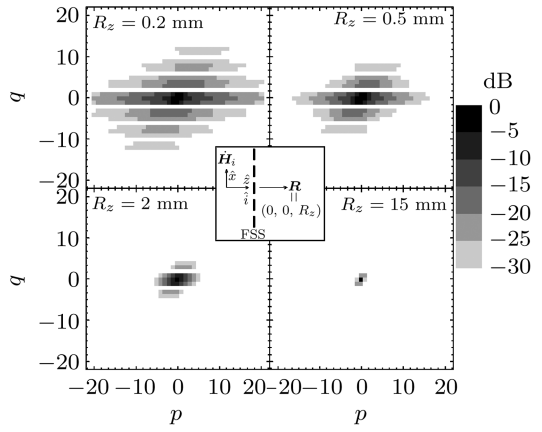


Fig. 5. The amplitude distribution of transmitted fields with respect to Floquet modes.

The explanation of the influence of air gaps is based on the above analyses. When the dielectric slab is fairly far from the FSS array, the modes of nonezero order as well as the dielectric boundary condition, have little influence on the FSS resonance characteristics, so its resonant frequency is similar to that of FSS in free space. When the dielectric slab is getting closer from far away, more and more orders of Floquet modes come into effects. The dielectric slab has changed the energy storage around the array, as well as the boundary condition, which exerts stronger influence on the transmission properties of the whole FSS structure. That means the loading effect is getting stronger. When the air gap vanishes, the resonant frequency decreases to the minimum. This explanation is essentially similar to the influence of supporting dielectric layers with different thickness on the transmission properties.[11]

3.3. A model of equivalent transmission line

As shown in Figs. 3 and 4, when $d_{\rm air}$ increases to more than $\lambda/5$, the resonant frequencies and the in-band transmission coefficients begin to change at a period of $\lambda/2$, and the amplitude of periodic changes depends on the thickness of dielectric slab. This phenomenon could be explained by a model of equivalent transmission line, as shown in Fig. 6. The two equivalent input admittances in the figure are respectively[12]

$$Y_{1+} = Y_\varepsilon \frac{Y_0 + \mathrm{j}Y_\varepsilon \tan\beta_\varepsilon d_\varepsilon}{Y_\varepsilon + \mathrm{j}Y_0 \tan\beta_\varepsilon d_\varepsilon}, \tag{4}$$

$$Y_{2+} = Y_0 \frac{Y_{1+} + \mathrm{j}Y_0 \tan\beta_0 d_{\rm air}}{Y_0 + \mathrm{j}Y_{1+} \tan\beta_0 d_{\rm air}}. \tag{5}$$

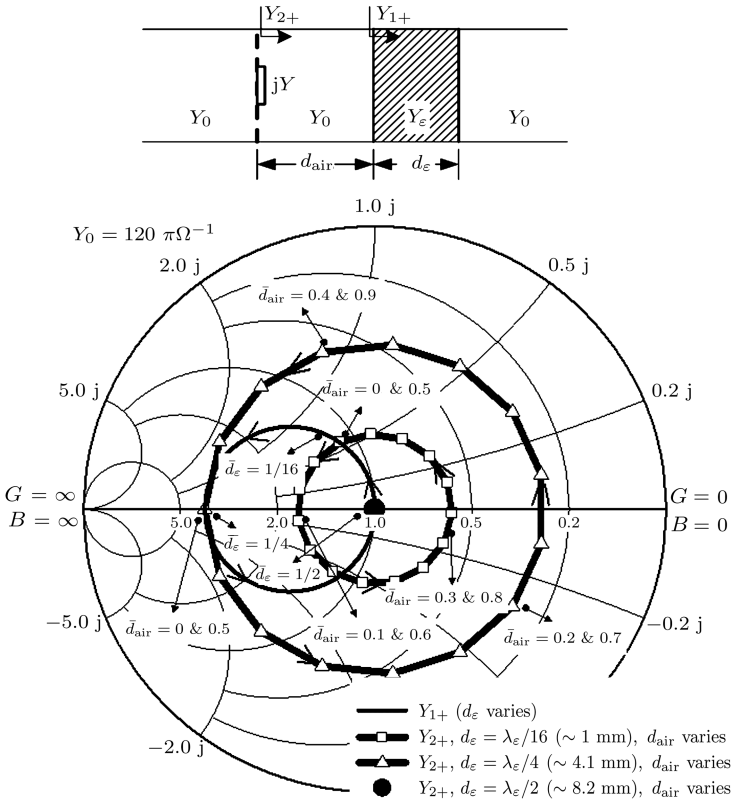


Fig. 6. The periodical change of equivalent input admittance.

Simplify it as a lossless transmission line, and set the dielectric parameter ε_r at 3.8 (tanδ equals 0). When Y_{1+} and Y_{2+} change with the thickness of dielectric slab and air gap, the loci could be illustrated in the Smith chart normalized to Y_0, the admittance in free space.

Y_{1+} changes periodically with the dielectric thickness d_ε, moving along the counter-clockwise direction on the circle of locus. When d_ε becomes half-wavelength $\lambda_\varepsilon/2$, the input admittance Y_{1+} equals Y_0, located at the centre of Smith chart, as shown in Fig. 6.

Y_{2+} contains two variables of d_ε and $d_{\rm air}$. Fix d_ε at three values: $\lambda_\varepsilon/16$, $\lambda_\varepsilon/4$ and $\lambda_\varepsilon/2$, corresponding to Figs. 3 and 4, then the changes of Y_{2+} with $d_{\rm air}$ are investigated in Fig. 6. Results show that Y_{2+} always changes periodically with $d_{\rm air}$ at a period of $\lambda/2$, which agrees with the periods of curves in Figs. 3 and 4. Furthermore, the magnitude of Y_{2+} is closely related to d_ε. When d_ε is the odd times of $\lambda_\varepsilon/4$, the distance between Y_{1+} and the chart centre is the largest, and the locus circle of Y_{2+} is the biggest, which means the most violent change with $d_{\rm air}$. Therefore, the resonance property changes most violently at $d_\varepsilon = 4.1$ mm in Fig. 3. When d_ε is the even times of $\lambda_\varepsilon/4$, Y_{1+} is located at the chat centre and the locus circle of Y_{2+} also shrinks to the central point, which means no change with $d_{\rm air}$. Therefore, the resonance property keeps constant at $d_\varepsilon = 8.2$ mm in Fig. 3. While d_ε is of other thickness, e.g. 1 mm, Y_{2+} would lie between the above two.

To sum up, when the resonance properties in Figs. 3 and 4 become steady, the changes of resonant frequencies and in-band transmission coefficients with air gaps match that of Y_{2+} in Fig. 6. As $d_{\rm air}$ is large enough, the influence of dielectric slab on transmission properties are mainly on the $0^{\rm th}$ order Floquet propagation mode. The boundary condition of admittance on the right-hand side of FSS array is the dominant factor that influences the resonance properties.

3.4. Discussion on the application of FSS technology

The bandpass radome is an important application of FSS technology. The principal rule in the design is to reduce the in-band transmission loss, so that the transmission performance meets the application requirements.[13] According to the above study on the influence of air gaps on the transmission properties of FSS structure, the most stable situation is at $d_\varepsilon = \lambda_\varepsilon/2$ and $d_{\rm air} \geq \lambda/5$, which leads to a stable resonant frequency and an in-band transmission coefficient. Furthermore, the in-band transmission loss of the FSS structure with suitable air gaps is obviously much lower than that of FSS structure loaded directly by dielectric without any air gaps.

A new concept of stealth shield radome is developed to improve the airborne nose radome of solid half-wavelength wall. An internal FSS shield radome could be fixed inside the solid wall radome, and it keeps a certain distance from its neighbouring ones. As long as the internal FSS shield radome is properly designed and the resonant frequency agrees with that of the external dielectric radome, the FSS technology could be conveniently applied to achieve the out-of-band stealth of radar cabin.

This concept is illustrated in Fig. 7. Set both the air gap and dielectric thickness at half-wavelength. The incidence parameters are set at TE polarization and 60° oblique incidence angle, corresponding to the typical condition in the design of airborne nose radome. In Fig. 7 $C_{\rm idp}$ means the product of the two independent transmission coefficients of the FSS screen (those in free space and the half-wavelength dielectric slab)

$$C_{\rm idp} = C_{\rm fsp} \times C_\varepsilon. \tag{6}$$

Results show that the transmission curve of the whole integrated structure containing air gaps ($C_{\rm int}$) agrees well with formula (6), i.e.,

$$C_{\rm int} \approx C_{\rm fsp} \times C_\varepsilon. \tag{7}$$

It shows the independence of the FSS array and the dielectric slab with the large air gaps. Furthermore, the resonant frequency and in-band transmission loss of the integrated structure are very close to that of the external half-wavelength radome. The in-band transmission coefficient approaches 90%, while that of the FSS structure loaded with the same dielectric with no air gap is lower than 75% (at the same resonant frequency). It shows that the design of stealth shield radome with air gaps could reduce the in-band transmission loss. The results in Fig. 7 also prove that the influences of the air gaps on transmission properties at oblique incidence are similar to the normal incidence as in Figs. 3 and 4.

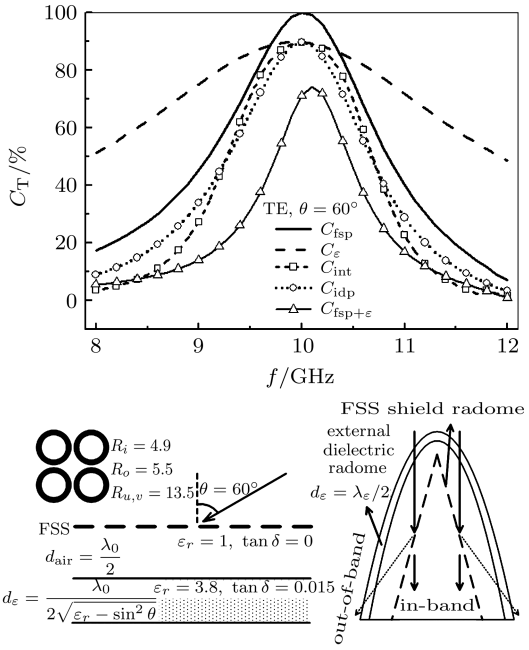


Fig. 7. The concept of FSS shield radome. $C_{\rm fsp}$: frequency response curve of the FSS array in free space; C_ε: frequency response curve of the dielectric slab of half wavelength; $C_{\rm int}$: frequency response curve of the integrated radome of dielectric slab and FSS shield radome with air gaps; $C_{\rm idp}$: frequency response curve of the product of two independent radomes; $C_{{\rm fsp}+\varepsilon}$: frequency response curve of the compound FSS structure with no air gaps designed for similar resonant frequency.

There are several advantages of the stealth shield FSS radome. Firstly, the transmission loss keeps low, approaching that of the external solid wall radome. Secondly, the cost of designing and manufacturing a shield FSS radome is much lower than redesigning a new FSS radome with complicated dielectric and shape. Finally, the mechanical and aerodynamic problems do not need much consideration any more in the design. What should be overcome in the application includes the out-of-band transmission properties, the arrangement and fixing inside the cabin and other potential deficiency.

4. Conclusion

In this paper, a detailed investigation was conducted about the influence of air gaps in the FSS structure. The results show that air gaps have a strong transmission property of FSS structure. Especially in the experimental study, even a 0.2-mm air gap may lead to a shift over 1 GHz in frequency. The transmission properties would change periodically with the air-gap thickness if it is larger than a specific value about $\lambda/5$. In the same period, the change of amplitude is related to the dielectric thickness. The dielectric of half-wavelength thickness exerts the slightest influence while the dielectric of a quarter-wavelength thickness exerts the strongest influence. Mechanism analyses and explanations were performed by Floquet mode analysis of the transmitted field, which indicate that the dielectric loading effect is exerted only on $0^{\rm th}$ order Floquet mode when the air gap is wide enough.

The concept of shielding radome for stealth can be introduced based on the above results and developed to improve the airborne radome of solid half-wavelength wall with narrow bandwidth. The FSS internal radome can be fixed inside the dielectric radome of solid half-wavelength wall with a certain distance, i.e. air gaps. Then the FSS technology could be conveniently applied to achieve the out-of-band stealth of radar cabin as long as the internal radome is properly designed and the resonant frequency agrees with that of dielectric radome. It presents a new thought for application of low loss FSS radomes at large incidence angle.

References

[1] Mittra R, Chan C H and Cwik T 1988 *Proceedings of the IEEE* **76** 1593

[2] Munk B A 2000 *Frequency Selective Surfaces*: *Theory and Design* (New York: John Wiley)

[3] Gao J S, Li X Q, Sun L C and Zhao J L 2008 *Acta Phys. Sin.* **57** 3803 (in Chinese)

[4] Jia H Y, Gao J S and Feng X G 2009 *Chin. Phys.* B **18** 1227

[5] Lu J, Sun G C and Wang J B 2009 *Chin. Phys.* B **18** 1598

[6] Wang H Q, Lü M Y and Wu Z 2005 *Journal of Infrared and Millimeter Waves* **24** 27 (in Chinese)

[7] Wang H Q, Lü M Y and Wu Z 2005 *Acta Electron. Sin.* **33** 1099 (in Chinese)

[8] Meng Z J, Huang J, Wu Z and Lü M Y 2008 *Optics and Precision Engineering* **16** 1247 (in Chinese)

[9] Vardaxoglou J C 1997 *Frequency Selective Surfaces*: *Analysis and Design* (London: Research Studies Press)

[10] Wu T K 1995 *Frequency Selective Surface and Grid Array* (New York: Wiley)

[11] Callaghan P, Parker E A and Langley R J 1991 *IEE Proceedings-H* **138** 448

[12] Radmanesh M M 2001 *Radio Frequency and Microwave Electronics Illustrated* (New Jersey: Prentice Hall)

[13] Walton J D 1970 *Radome Engineering Handbook: Design and Principles* (New York: M. Dekker)